Optimized Reconfigurable UWB Monopole with WLAN Band Notch Using C-Shape slot & MEMS Stubs

Bhanu Pratap[1], Navjot Kaur [2], Swati Sharma[3]

[1,2,3] Universal Institute of Engineering & Technology, Lalru Punjab India

[1]bhanupratap96@gmail.com

***Abstract*— Two CPW-fed trapezium monopoles were designed on FR4 substrate, dielectric constant is 4.4 with height 1 mm and 26*30 mm^2 plane area with reconfigurable rejection band (band-notch) characteristics in the frequency range between 5 and 6 GHz. The first antenna uses a λ/2 long, C-shaped slot and the second antenna uses two symmetrically placed λ/4 long, inverted L-shaped stubs as resonating elements. Microelectromechanical system (MEMS) switches are used to activate and deactivate the resonating elements without the need of dc bias lines due to use of a novel MEMS switch. Surface current distributions are used to explain the effect of the additional resonating elements. Reflection coefficient radiation pattern and gain measurements are presented to verify the design concepts featuring a very satisfactory performance. The antenna shows satisfactory gain uniformity with stable omnidirectional radiation patterns across the UWB bands (3.1 to 10.6).**

***Index Terms*—Electromagnetic analyses, coplanar waveguide (CPW) fed antennas, integrated antenna, phase linearity, ultrawideband (UWB), microelectromechanical system (MEMS), reconfigurable,**

I. INTRODUCTION

Since the rapidly increasing number of wireless applications has led to a very heavy congestion in the available RF and wireless spectrum, causing significant interference among the different users and degrading the performance of the affected radios. To overcome this problem in an opportunistic way, agile radios are required [1] that demand the use of "smart," reconfigurable antennas capable of canceling in-band interference. Since the ultrawideband (UWB) radios share part of the spectrum with the HIPERLAN/2 applications (5.15–5.35 GHz, 5.470–5.725 GHz) and the wireless local area network (WLAN) applications using the IEEE 802.1la (5.15–5.35 GHz, 5.725–5.825 GHz) protocol, an UWB antenna with reconfigurable band-rejection characteristic at the WLAN frequencies is highly desirable.

Over the nominated bandwidth of UWB system, several designs of UWB antennas with band rejection characteristics have been investigated and successfully implemented in the past. Two parasitic patches were used in [2], two linear slots were used for the Vivaldi antenna presented in [3] and the printed log-periodic antenna presented in [4], while a split ring resonator (SRR) was added on the microstrip-fed monopole suggested in [5]. However none of those antennas had reconfigurable band-notch characteristics. Some antennas with endogenous band-notch characteristics were also introduced, like the λ/4 combined monopoles [6], the monopole with the integrated filter [7], the sail-boat antenna presented in [8] and the fractal antenna proposed in [9]. Two open-circuit stubs were used in [10], in an approach similar to one of the two solutions suggested in the present paper. However, the technique that was adopted by most researchers was the integration of a U-shaped slot on a monopole [11]–[14] or the integration of stubs with the monopole [15]. Numerous researchers have integrated Microelectromechanical system (MEMS) switches and antennas to develop frequency [16], [17] or radiation pattern [18] reconfigurable antennas. In all those cases, the MEMS switches were actuated using dc bias lines.

In this paper, two UWB monopole antennas with an integrated MEMS switch that can be actuated to place a stopband at the HIPERLAN/2 and WLAN frequencies are demonstrated. The MEMS switches are used so that they do not require extra bias lines; the bias is applied to the RF signal line. The lack of bias lines for the MEMS switches in the proposed design makes the fabrication easier and improves the radiation performance of the antenna since there is no coupling or leakage from the bias lines. For the first antenna, a C-shaped slot is placed within the monopole to achieve the band rejection properties. For the second antenna, two inverted L-shaped open circuit stubs are symmetrically placed near the elliptical radiator and MEMS switches connect them to the radiator when the band rejection is required. In the following sections, the antennas design is given first, and then their operation and design are confirmed through simulations.

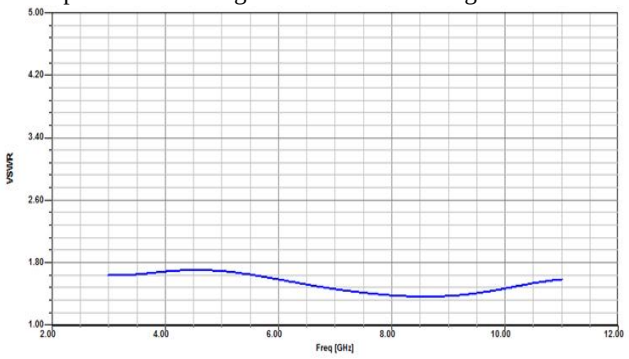

Fig. 1 Simulated VSWR of Fig. 2 (a) with optimal dimensions.

On based the background of the researches above the proposed antenna designed with C-shape slots in radiating patch with half wavelength which are responsible the needed notch frequency 5.5 GHz. The forward segment of the feed has the advantage of compact size compared with existing antenna [23] and without much adjustment the existing structure can be used for notched design. The antenna is simulated and analyzed by using simulation software, Ansoft HFSS.

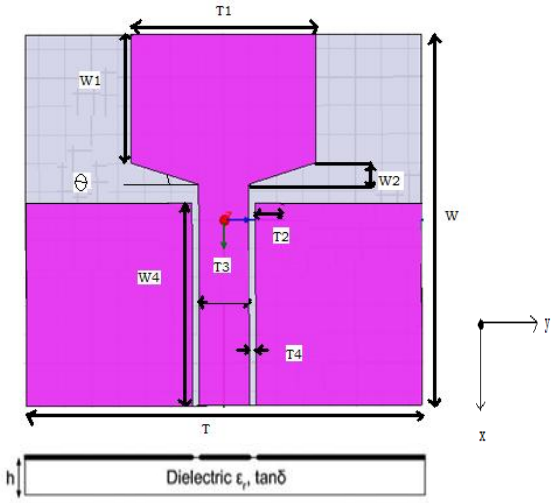

(a)

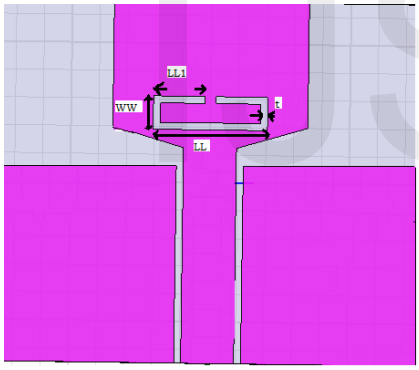

(b)

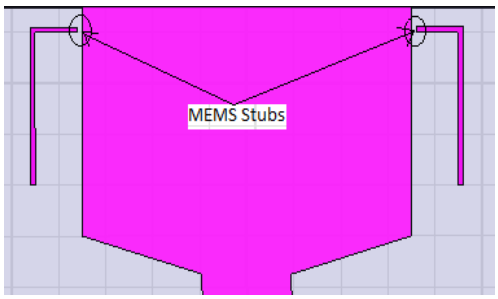

(c)

Fig. 2 (a), (b) and (c): Antenna with optimized dimensions (a) Without slot (b) With C-shape slot (c) with L-shape slot.

II.ANTENNA DESIGNS AND RESULT DISCUSSION

In the design of fig. 2 (a), (b) and (c), the length 'T' and width 'W' play an important role to determining the resonant frequency of the system. The initial values of these parameters are taken approximately one wavelength of center frequency (6.85 GHz) for the substrate height (h=1mm), dielectric constant (ε_r=4.4) and loss tangent d=0.02. Both the radiating patch and the ground plane are beveled, which results in a smooth transition from one resonant mode to another and ensures good impedance match over a broad frequency range [7], [8]. The design of the UWB rhomboid antenna starts with choosing T1, W1. T1 and W1 are critical parameters associated with the upper and lower operating frequencies of the antenna. W1, on the other hand, is a key parameter to maintain good input impedance for the frequency range of 3.1–11 GHz. Accordingly, T1 and W1 are selected to have a reasonable VSWR at f_{min}=3.1 GHz and f_{max}=11.6 GHz, which are the lower and upper ends of the UWB band. A fine starting point for these dimensions is as follows:

$$W1 \approx \lambda_{e,fmax}/4 \quad (1)$$

$$T1+W1 \approx \lambda_{e,fmin}/4 \quad (2)$$

Where $\lambda_e=\lambda_0/\sqrt{\varepsilon_e}$ is the effective wavelength for the radiation mode in the FR-4 substrate with the effective dielectric constant (ε_e=1.02≈1 for the 1mm FR-4 substrate). $\lambda_{e,fmax}$ and $\lambda_{e,fmin}$ are the effective wavelengths at the upper and lower UWB frequencies, respectively. W1 is chosen to obtain reasonable return loss values for the whole frequency band. In particular, the optimization of W1 is critical for obtaining a good match at the high end of the UWB spectrum.

The calculated values of the antenna are optimized with HFSS tool. The optimization has been done to perform for the most excellent impedance bandwidth. For design presented in the paper, the effective length of the c-shaped slots in the radiating patch is approximately 0.5 times of wavelength of frequency 3.5 GHz and 5.5 GHz respectively. The final parameters of fig.2 (a) are T=30mm, T1=14mm, T2=1.8mm, T3=3.8mm, T4=0.5mm, W=42mm, W=26mm, W1=9mm, W2=1.5mm, W3=9.2mm, W4=14.7mm; slot dimensions of the single notch in fig 2(b) are LL1=3mm, LL=8mm, WW=2.6mm and t=0.5mm.The other dimensions which are not shown in fig 2. (b) Are same as in fig 2. (a).

Two MEMS switches are used to electrically connect and disconnect the two stubs to the trapezium radiator. The switches are positioned 0.4 mm from the trapezium. Bias lines are not needed in neither the slot nor the stubs case for the MEMS switch actuation because of the switch topology [21].

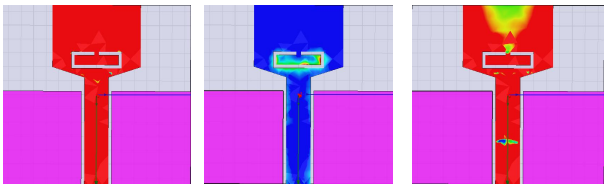

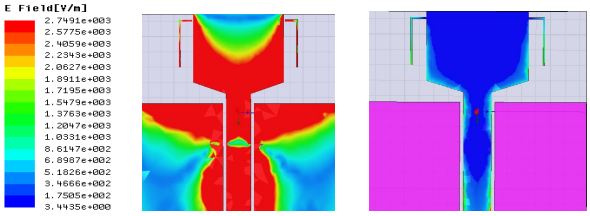

Fig. 3 shows the current distribution of antenna at different-2 frequencies, (a) at 3 GHz, (b) at 5.5 GHz, (c) at 8 GHz, (d) at 5.5 GHz for open stubs, (e) at 5.5 GHz for short stubs & (f) at 8 GHz for short stubs

Fig.2 shows the configuration of the proposed monopole antenna it consist a trapezium radiating patch with C-slot and CPW fed with rectangular ground plane. Fig.4 shows the simulated VSWR with shorted stubs and with slot in radiating patch. The radiating patch has a strong significant effect on the antenna's bandwidth enhancement which is depicted by Fig. 1.

Fig.3 shows the simulated current distributions at different frequencies. In Fig. 3(a) and (c), at frequencies 3 and 8 GHz, the current distributions mainly flow along the transmission line, while around the C-shaped slot the current is small. At 5.5 GHz as shown in Fig.3 (b), destructive interference for the excited surface currents in the antenna will occur, which causes the antenna to be nonresponsive at that frequency. Similarly For the open stubs antenna, the two L-shaped, open circuit terminated stubs Fig.3 (d) have a length approximately λ/4 at 5.5 GHz resulting in resonating elements that prevent radiation if the MEMS switches are down or closed, which connects the stub to the monopole. The impedance nearby the feed-point changes acutely making large reflection at the desired notched frequency.

As a result, the antenna does not radiate at that frequency and a frequency notch is created around the frequency of 5.5 GHz. When the stubs is shorted at its center point by the MEMS switch, the total length of the stubs is divided in two and, consequently, it cannot support the resonating currents; thus, radiation occurs as if the stubs was not present. A simple transmission line model, similar to the approach introduced in [19], is presented in Fig.3 that explains the slot effect. The presence of the stubs is modeled as a λ/4 long, short circuit terminated series stub, which is similar to a spurline filter. The MEMS switch is across the input to the series stub. If the switch is up, [Fig.3 (a)] the spurline filter is in the circuit, and at the stub resonant frequency, there is an equivalent series open circuit that reflects the signal. However, if the switch is down, the spurline filter is shorted [Fig.3 (b)], or not in the circuit. Thus, radiation occurs at all frequencies.

The notch frequency given the dimensions of the band notched characteristic can be given as

$$f_{notch}=C/2L\sqrt{\varepsilon_e} \qquad 3$$

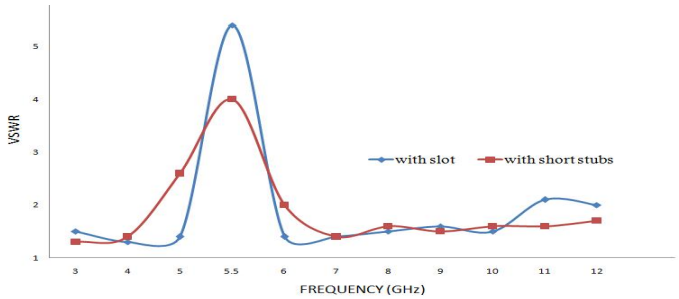

Fig. 4 Simulated VSWR of antenna (Fig. 2 (b, c)) with optimal dimensions

To better understand the behaviour of the antenna, in UWB resonances, Fig. 4 shows the comparison of VSWR of antenna (b), (c).

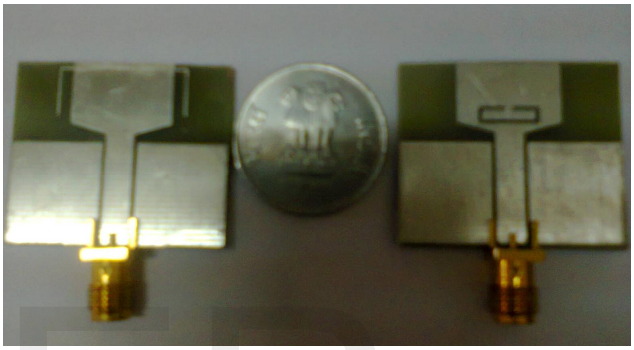

Fig.5 Fabricated design

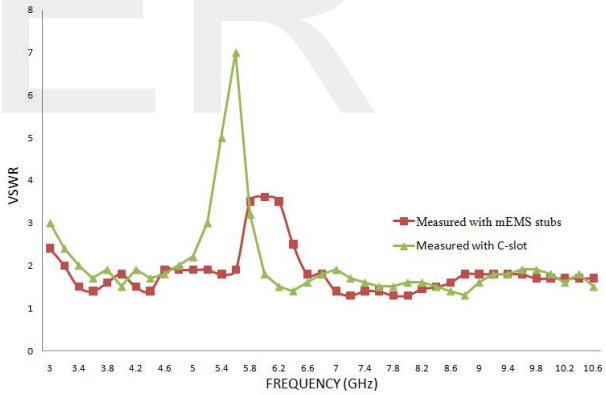

Fig. 6 Measured VSWR of antenna (Fig. 2 (b, c)) with optimal dimensions

As UWB system uses pulse communication, a key matter is pulse distortion by the antenna. Ideally, a linear phase response (constant group delay) is required. Fig. 7 describes the simulated group delay of antenna 2(b) and antenna 2(c). The variation of the group delay of antenna (a) over the UWB band is less than 1ns. The group delay variations of antenna (b) highly exceed 4 ns in the area of notch band (5-6 GHz), similarly for band notch (antenna c) is also having highly group delay variations (4ns) at notch band area (5-6 GHz) respectively which can depreciate phase

linearity. However, in the un-notched frequency part, the group delay variations are minute showing good quality characteristics. These group delay characteristics demonstrate that the proposed antennas exhibit phase linearity at required UWB frequencies.

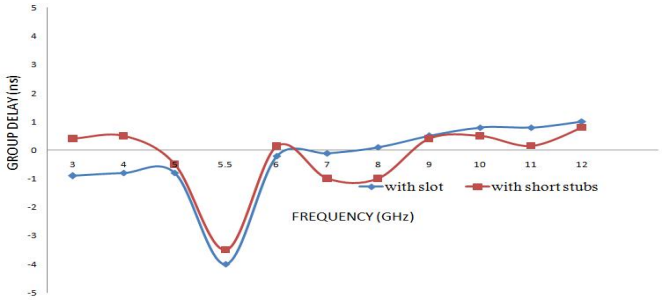

Fig. 7. Simulated group delay of antenna 2(b) and 2(c)

The last parameter is the radiation pattern of the antenna. This parameter is highly dependent on the application of the antenna. In the case of the antenna our group designed, we had to have an omnidirectional radiation pattern. This means that the radiation pattern had to be spread evenly 360 degrees around the antenna. The reason for this is because since the location of the transmitter is not fixed, you want to spread the radiated signal out as far as possible so the receiver will be able to pick up the transmitted signal.

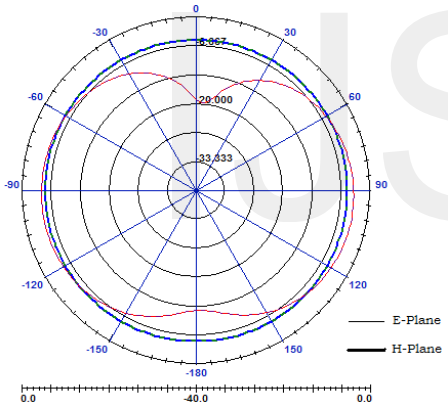

(a)

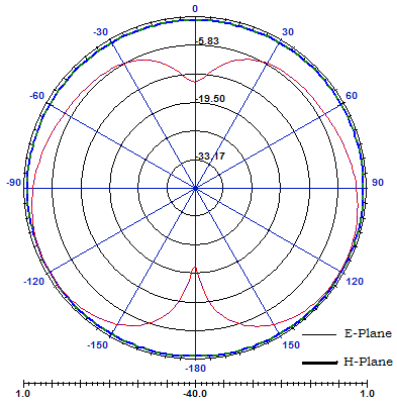

(b)

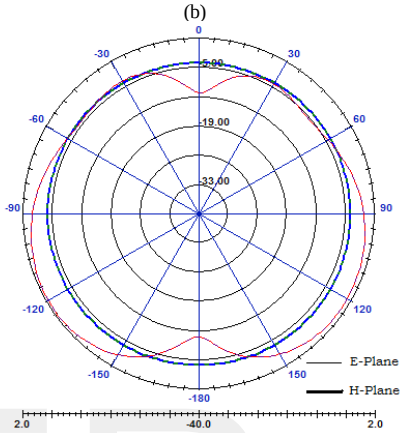

(c)

Fig. 8. Simulated radiation far-field patterns for the proposed antenna 2 (c) operation at (a) 3 GHz, (b) 8 GHz, and (c) 10 GHz

For briefness, the simulated E-plane and H-plane radiation patterns at 3, 8 and 10 GHz are shown in Fig. 8 (a), (b) and (c) respectively. It is seen that this antenna has the almost omni-directional radiation pattern like normal monopole antennas. However, the omni-directional radiation properties have a little deterioration as frequency. Over the entire bandwidth, it is similar to a conventional wideband monopole antenna.

IV. Conclusions

The use of resonating elements integrated with MEMS switches has been exploited to implement two UWB monopoles with reconfigurable band notch in the WLAN frequency range (4.85–6.2 GHz). The basic antenna design is a trapezium radiator fed with CPW line. In the initial case a C-shaped slot of approximate λ/2 length causes the frequency notch. In the second case, two inverted L-shaped open stubs are used and two MEMS switches are used to connect and disconnect the stubs with the trapezium radiator. The electrical connection of the stubs with the radiator causes the creation of the rejection band and, apparently, when the stubs are not electrically connected, the antenna operates as a typical UWB radiator with radiation band that covers the whole UWB range (3.1–10.6 GHz). Reconfigurability is achieved with MEMS switches that are actuated through the RF signal path, without the need of dc bias lines, that could

potentially complicate the switch fabrication and integration process, while degrading the radiation performance of any antenna and especially of a broadband antenna because RF leakage through the bias lines cannot be avoided. Numerical results, transmission line models and eventually measurements verify the very satisfactory performance of the proposed antennas which can be good candidates for next generation, high performance and high versatility cognitive radios.

REFERENCES

[1 S. Haykin, "Cognitive radio: Brain-empowered wireless communications," *IEEE J. Select. Areas Comm.*, vol. 23, pp. 201–220, Feb. 2005.

[2] K.-H. Kim, Y.-J. Cho, S.-P. Hwang, and S.-O. Park, "Band-notched UWB planar monopole antenna with two parasitic patches," *Electron. Lett.*, vol. 41, no. 14, pp. 783–785, Jul. 7, 2005.

[3] I.-J. Yoon, H. Kim, and Y. J. Yoon, "UWB RF receiver front-end with band-notch characteristic of 5 GHz WLAN," in *IEEE Int. Antenna Propag. Symp. Digest*, Jul. 2006, pp. 1303–1306.

[4] S.-Y. Chen, P.-H. Wang, and P. Hsu, "Uniplanar log-periodic slot antenna fed by a CPW for UWB applications," *IEEE Antenna Wireless Propag. Lett.*, vol. 5, no. 1, pp. 256–259, Dec. 2006.

[5] J. Kim, C. S. Cho, and J. W. Lee, "5.2 GHz notched ultra-wideband antenna using slot-type SRR," *Electron. Lett.*, vol. 42, no. 6, pp. 315–316, Mar. 16, 2006.

[6] K. Chang, H. Kim, and Y. J. Yoon, "Multi-resonance UWB antenna with improved band notch characteristics," in *IEEE Int. Antenna Propag. Symp. Digest*, Jul. 2005, vol. 3A, pp. 516–519.

[7] S.-W. Qu, J.-L. Li, and Q. Xue, "A band-notched ultrawideband printed monopole antenna," *IEEE Antenna Wireless Propag. Lett.*, vol. 5, no. 1, pp. 495–498, Dec. 2006.

[8] S.-Y. Suh, W. L. Stutzman, W. A. Davis, A. E. Waltho, K. W. Skeba, and J. L. Schiffer, "A UWB antenna with a stop-band notch in the 5-GHz WLAN band," in *Proc. IEEE ACES*, Apr. 2005, pp. 203–207.

[9] W. J. Lui, C. H. Cheng, and H. B. Zhu, "Compact frequency notched ultra-wideband fractal printed slot antenna," *IEEE Microw. Wireless Comp. Lett.*, vol. 16, no. 4, pp. 224–226, Apr. 2006.

[10] W. J. Lui, C. H. Cheng, and H. B. Zhu, "Frequency notched printed slot antenna with parasitic open-circuit stub," *Electron. Lett.*, vol. 41, no. 20, pp. 1094–1095, Sep. 29, 2005.

[11] T. Dissanayake and K. P. Esselle, "Design of slot loaded band-notched UWBantennas," in *IEEE Int. Antenna Propag. Symp. Digest*, Jul. 2005, vol. 1B, pp. 545–548.

[12] A. J. Kerkhoff and L. Hao, "Design of a band-notched planar monopole antenna using genetic algorithm optimization," *IEEE Trans. Antennas Propag.*, vol. 55, no. 3, pt. 1, pp. 604–610, Mar. 2007.

[13] K. Chung, J. Kim, and J. Choi, "Wideband microstrip-fed monopole antenna having frequency band-notch function," *IEEE Microw. Wireless Comp. Lett.*, vol. 15, no. 11, pp. 766–768, Nov. 2005.

[14] Y. J. Cho, K. H. Kim, D. H. Choi, S. S. Lee, and S.-O. Park, "A miniature UWB planar monopole antenna with 5-GHz band-rejection filter and the time-domain characteristics," *IEEE Trans. Antennas Propag.*, vol. 54, no. 5, pp. 1453–1460, May 2006.

[15] Y.-C. Lin and K.-J. Hung, "Compact ultrawideband rectangular aperture antenna and band-notched designs," *IEEE Trans. Antennas Propag.*, vol. 54, no. 11, pt. 1, pp. 3075–3081, Nov. 2006.

[16] D. E. Anagnostou, G. Zheng, M. T. Chryssomallis, J. C. Lyke, G. E. Ponchak, J. Papapolymerou, and C. G. Christodoulou, "Design, fabrication, and measurements of an RF-MEMS-based self-similar reconfigurable antenna," *IEEE Trans. Antennas Propag.*, vol. 54, no. 2, pt. 1, pp. 422–432, Feb. 2006, J..

[17] A. C. K. Mak, C. R. Rowell, R. D. Murch, and C. L. Mak, "Reconfigurable multiband antenna designs for wireless communication devices," *IEEE Trans. Antennas Propag.*, vol. 55, no. 7, pp. 1919–1928, Jul. 2007.

[18] C. W. Jung, M.-J. Lee, G. P. Li, and F. De Flaviis, "Reconfigurable scan-beam single-arm spiral antenna integrated with RF-MEMS switches," *IEEE Trans. Antennas Propag.*, vol. 54, no. 2, pt. 1, pp. 455–463, Feb. 2006.

[19] W.-S. Lee, D.-Z. Kim, K.-J. Kim, and J. W. Yu, "Wideband planar monopole antennas with dual band-notched characteristics," *IEEE Trans. Microw. Theory Tech.*, vol. 54, no. 6, pt. 2, pp. 2800–2806, Jun. 2006.

[20] B. Kim, S. Nikolaou, D. E. Anagnostou, Y. S. Kim, M. M. Tentzeris, and J. Papapolymerou, "A conformal L-shaped antenna on liquid crystal polymer substrate for ultra-wideband systems with WLAN band-stop characteristics," *IEEE Trans. Antennas Propag.*, submitted for publication.

[21] N. Kingsley, D. E. Anagnostou, M. M. Tentzeris, and J. Papapolymerou, "RF MEMS sequentially-reconfigurable Sierpinski antenna on a flexible, organic substrate without the need for dc bias lines," *IEEE Trans. Antennas Propag.*, submitted for publication.

[22] A. D. Yaghjian, "Approximate formulas for the far field and gain of open-ended rectangular waveguide," *IEEE Trans. Antennas Propag.*, vol. AP-32, no. 4, pp. 378–384, Apr. 1984.

[23] Symeon Nikolaou, , Nickolas D. Kingsley, George E. Ponchak,, John Papapolymerou and Manos M. Tentzeris, *Senior Member, IEEE IEEE Trans. on Antennas and Propag., vol. 57, no. 8, august 2009'*